

Accelerate cycle expansions by dynamical conjugacy

Ang Gao,^{1,*} Jianbo Xie,^{1,2} and Yueheng Lan^{1,†}

¹*The Department of Physics, Tsinghua University*

²*The Department of Physics, UC Berkeley*

The periodic orbit theory provides two important functions—the dynamical zeta function and the spectral determinant—to calculate dynamical averages for an ergodic dynamical system. For hyperbolic systems, the cycle expansions for the two functions converge rapidly. However, for non-hyperbolic systems, the convergence of cycle expansions is slowed down. We compare the convergence of the dynamical zeta function and the spectral determinant for one-dimensional maps and show for maps with critical points, the convergence is much slower than that in the hyperbolic case. By the dynamical conjugacy, we can clear out the influence of critical points and accelerate the convergence for cycle expansions.

I. INTRODUCTION

Although equilibrium statistical physics has been extremely successful, the accurate computation of physical averages in non-equilibrium systems remains to be a great challenge both analytically and numerically, due to the difficulty of procuring the statistical weight based on the equation of motion that governs the state evolution [5, 16]. From a dynamical systems point of view, this weight is equivalent to the natural measure in the phase space, which often is not smooth or even singular for a chaotic system [14, 22]. Periodic orbit theory (POT) avoids a direct description of this possibly fractal measure by expressing phase space averages in terms of averages on periodic orbits or cycles and thus is a powerful way for reliable and accurate characterization [7, 15, 20, 23]. The associated cycle expansion of spectral determinant or dynamical zeta function orders cycles in a hierarchical way such that dynamical averages are dominated by a few short cycles and the long ones give decreasing corrections. For a uniformly hyperbolic system with finite symbolic dynamics, the corrections decrease exponentially or even super-exponentially [1, 17, 21]. However, for non-hyperbolic systems, the convergence could be extremely poor, undermining the applicability of cycle expansions [7].

Many real physical systems are non-hyperbolic. For example, in an intermittent system, typical trajectories alternate between regular and chaotic motions in an irregular way and thus cause non-hyperbolicity [3, 11]. A milder type of non-hyperbolicity is created by the strong contraction at

specific points such as homoclinic tangencies or critical points in 1-d maps [1, 2]. At these points, the natural measure becomes non-analytic and thus the nice shadowing property among cycles that is necessary for fast convergence of cycle expansions fades out. Poles appear near the origin in the dynamical zeta function and the spectral determinant which is not entire any longer. To compute averages with fair accuracy, many orbits are needed, which usually requires unaffordable amount of resources. Thus, how to accelerate the convergence of cycle expansions in the presence of non-hyperbolicity is a central problem in practical applications.

Several accelerating schemes have been proposed based on the analyticity of the spectral functions. One idea is to identify and remove the poles that are near the origin and thus expand the radius of convergence. In [1, 2, 4], the dominant terms in the tail of the expansion are estimated and summed to approximately evaluate the leading pole. More accurate estimation is obtained by using Padé approximation, which is valid not only for the leading pole but also for other poles [13, 18]. An interesting consequence of analyticity of the underlying dynamics is the existence of infinite sum rules which indicates the strong correlations among the stabilities of periodic orbits. These exact relations show redundancy of information embedded in the periodic orbit and can be used to accelerate the convergence of cycle expansions [19]. In certain cases, the analyticity can be utilized to derive the spectral function with no resort to periodic orbits and thus implies a potential interesting route to the spectrum computation. But so far, it succeeded only for several very specific maps and hard to be utilized in more general case [8].

In this paper, we mainly employ a geometric picture of the cycle expansion to treat the convergence problem [6, 9]. Maps with critical points have a nat-

* E-mail: ang.dionysos.gao@gmail.com

† E-mail: lanyh@mail.tsinghua.edu.cn

atural measure with singularities, due to the strong contraction around critical points. This contraction also deteriorates the shadowing between cycles and thus leads to the bad convergence of cycle expansions. So, the singularity in the natural measure is an effective indicator of unbalance of cycle weights and leads to small radius of convergence. One idea to improve the convergence is to clear out singularities in the natural measure. In the current paper, we achieve this by properly designing coordinate transformations such that the resulted conjugate map has a natural measure with no singularity. The computation of dynamical averages for the original map can be efficiently done with the counterparts for the conjugate map since the convergence is much improved in the new map.

In the following, after a brief review of periodic orbit theory in Section II, we discuss the convergence of the dynamical zeta function and the spectral determinant for maps with critical points in Section III. An comparison between spectral functions is made and the importance of hyperbolicity in calculation is emphasized. With a description of the geometric significance of the truncation in cycle expansion, our accelerating scheme is presented and tested in several examples. In Section IV, we summarize the paper and discuss the remaining problems and possible future direction for further investigation.

II. PERIODIC ORBIT THEORY

For map $f : \mathcal{M} \rightarrow \mathcal{M}$ and observable $a(x)$, we can define the evolution operator \mathcal{L}^n , the kernel of which is

$$\mathcal{L}^n(y, x) = \delta(y - f^n(x))e^{\beta A^n}, \quad (1)$$

where β is an auxiliary variable and $A^n = \sum_{k=0}^{n-1} a(f^k(x))$. We can obtain the average $\langle a \rangle$ through the leading eigenvalue of \mathcal{L} . Suppose the leading eigenvalue of \mathcal{L} is e^{s_0} , then we have

$$\langle a \rangle = \frac{\partial s_0}{\partial \beta} \Big|_{\beta=0}. \quad (2)$$

At a special case, when $\beta = 0$, we have $\mathcal{L}^n(y, x) = \delta(y - f^n(x))$, which is the kernel of the so called Perron-Frobenius operator. The escape rate of the dynamical system, which we denote by γ , can be obtained through the leading eigenvalue of this operator

$$\gamma = -s_0. \quad (3)$$

The eigenvalues of the evolution operator \mathcal{L} can be detected by means of the spectral determinant, which is related to the trace of \mathcal{L} and thus to the periodic orbits by the identity

$$\ln \det(1 - z\mathcal{L}) = \text{Tr} \ln(1 - z\mathcal{L}). \quad (4)$$

For one-dimensional maps, it can be written as

$$\det(1 - z\mathcal{L}) = \exp\left(-\sum_p \sum_{r=1}^{\infty} \frac{1}{r} \frac{z^{n_p r} e^{r\beta A_p}}{|1 - \Lambda_p^r|}\right), \quad (5)$$

where p denotes prime cycles which cannot be expressed with repeats of shorter cycles, Λ_p is the stability eigenvalue of cycle p and n_p is its length. In most applications, we are only interested in the leading eigenvalue. It is obvious that the smallest positive zero of the spectral determinant is e^{-s_0} , the inverse of the leading eigenvalue of \mathcal{L} . In view of Eq. (2), we can obtain dynamical averages through the spectral determinant.

The leading eigenvalue can alternatively be obtained from a simpler spectral function—the dynamical zeta function

$$\frac{1}{\zeta} = \prod_p (1 - t_p), t_p = \frac{1}{|\Lambda_p|} z^{n_p} e^{\beta A_p}. \quad (6)$$

It can be proved that $\frac{1}{\zeta}$ is the zeroth-order approximation of the spectral determinant and they have the same smallest positive zero. Most often, however, their analyticity is different.

Practically, to evaluate the zeros, we expand the spectral determinant or the dynamical zeta function in terms of power series and get polynomials through truncation. The power series expansion is known as cycle expansion. For example, for the one-dimensional map with complete binary symbolic dynamics, the dynamical zeta function can be expanded as

$$\frac{1}{\zeta} = 1 - t_0 - t_1 - [(t_{01} - t_0 t_1)] - [(t_{001} - t_{01} t_0) + (t_{011} - t_{01} t_1)] - \dots \quad (7)$$

If we keep only the terms explicitly shown in Eq. (7), the cycle expansion is truncated at cycle length 3 and resulting in a polynomial in z of degree 3. The linear term is the fundamental contribution which gives the dominant part of the expansion. Higher order terms are curvature corrections which consist of contributions from prime cycles such as t_{01} and from pseudo-cycles being combination of prime cycles such as $t_0 t_1$. The cancelation between them signals the shadowing properties and the analyticity

of the system and results in an exponential decrease of the curvature corrections when uniform hyperbolicity is guaranteed. However, there is no good cancellation in the presence of non-hyperbolicity and cycle expansion converges very slowly. We are trying to restore this cancellation by dynamical conjugacy under certain circumstance.

Besides the dynamical zeta function and the spectral determinant, there are two other ways to obtain the dynamical average. One way is through the time averaging, which is defined as

$$\overline{a(x_0)} = \frac{1}{N} \sum_{i=0}^N a(x_i), \quad (8)$$

where $x_0 \rightarrow x_1 \rightarrow \dots \rightarrow x_N$ is an itinerary generated by the map $f(x)$ and N is a number large enough. For an ergodic system, if the initial point x_0 is not a periodic orbit point, we have

$$\langle a \rangle = \overline{a(x_0)}, \quad (9)$$

which means the time averaging can be used to calculate the average.

Another way to obtain average $\langle a \rangle$ is through a phase space average. For the map $f(x)$, when $n \rightarrow \infty$, any smooth measure will approach an invariant measure, called the natural measure. More formally,

$$\rho(x) = \lim_{n \rightarrow \infty} \int_{\mathcal{M}} dy \delta(x - f^n(y)) \rho_0(y), \quad \int_{\mathcal{M}} dy \rho_0(y) = 1, \quad (10)$$

where $\rho(x)$ is the natural measure and $\rho_0(y)$ is the initial smooth measure. With the natural measure, the average $\langle a \rangle$ can be obtained by

$$\langle a \rangle = \int_{\mathcal{M}} a(x) \rho(x) dx, \quad (11)$$

which implies an alternative way to achieve the average.

III. IMPROVING THE CONVERGENCE OF CYCLE EXPANSIONS

A. Numerical computation methods we used

To obtain the dynamical averages, we need to build the truncated dynamical zeta function and spectral determinant. The method to get these is discussed in detail in [7]. If we impose a cutoff of order N , we need to drop out all the cycles longer than N , and we call N the truncation length. To study

the convergence of cycle expansions, we evaluate the escape rate and other dynamical averages with the truncated dynamical zeta function and spectral determinant. Also, we investigate the dependence of computational errors of physical averages on the truncation length. However, except for very few cases, we have no idea of the exact values of averages. In practice, when we calculate errors with the truncation length no larger than N_{\max} , we use averages obtained with the truncation length $N_{\max} + 1$ as the exact value. Many figures are plotted to monitor this dependence. Note the logarithm scale in the ordinate.

We also compute the natural measure produced by map iterations. We choose a random initial point and iterate it many times, usually 10^7 if not specified otherwise. Then, by counting the times that the point enters a small interval, we can get a probability distribution, which is the natural measure for an ergodic system. As the maps discussed in this paper are all ergodic, though not that accurate in some cases, this method is good for calculating the natural measure. In addition, with Eq. (8), we can get physical averages with this iterations at the same time.

B. Comparison of the dynamical zeta function and the spectral determinant

The escape rate and other dynamical averages may be evaluated with the dynamical zeta function or the spectral determinant. However, the convergence rates of the two methods are quite different. The difference is due to the difference in their radius of convergence in cycle expansions. To show this, we calculate the escape rate of the map $f(x) = 6x(1 - x)$, $\mathcal{M} = [0, 1]$, $f: \mathcal{M} \rightarrow \mathcal{M}$ with the dynamical zeta function and the spectral determinant. The results are listed in TABLE I.

From the table, we can see that both methods converge fast, thanks to the nearly perfect cancellation between the prime cycles and the pseudo-cycles. Thus we get very accurate results with only several short prime cycles. Moreover, we see that the results computed with the spectral determinant converges much more quickly than with the dynamical zeta function, implying a difference in their analyticity.

FIG. 1 shows the dependence of the error in the computed escape rate on the truncation length N with the dynamical zeta function and the spectral determinant respectively. It is clear that the logarithm of the error decreases linearly for the dynamical zeta function and super-linearly for the spec-

N	$\gamma(\frac{1}{\mathcal{L}})$	$\gamma(\det(1 - z\mathcal{L}))$
1	0.87	0.9
2	0.83	0.83
3	0.83151	0.831492
4	0.831492	0.831492987
5	0.831493012	0.831492987487621
6	0.831492987	0.831492987487621617307
7	0.8314929875	0.8314929874876216173072762950
8	0.831492987487	0.83149298748762161730727629503691
9	0.8314929874876	
10	0.83149298748762	

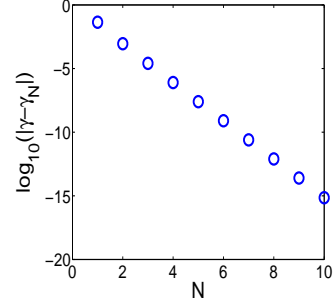
TABLE I. Escape rate obtained by the dynamical zeta function $\frac{1}{\mathcal{L}}$ and the spectral determinant $\det(1 - z\mathcal{L})$

tral determinant, which suggests that the error decreases exponentially for the dynamical zeta function and super-exponentially for the spectral determinant. One possible reason for this difference is that the spectral determinant is analytic over the whole complex plane, while the dynamical zeta function is only analytic in a region with a finite radius. Thus, the coefficient of the N th-order term decreases super-exponentially with N in the spectral determinant, and exponentially in the dynamical zeta function. The different way the coefficient of the N th-order term decreases determines their different convergence rate. The analyticity is the essential factor that results in the difference.

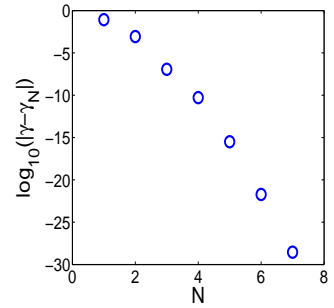
C. The influence of hyperbolicity

Having compared the convergence rate of the dynamical zeta function and the spectral determinant for the map $f(x) = Ax(1 - x)$, with $A = 6$, we check how the value of A influence the convergence rate.

Firstly, we set A equal to 5 and repeat the above computation for the escape rate, the results are shown in FIG. 2. We see that though a little slower than the $A = 6$ case, both methods converge fast—the dynamical zeta function method converges nearly exponentially and the spectral determinant exhibits a beautiful super-exponential convergence, just like what happened before. It looks as if the change of A had little effect on convergence. However, if we set A equal to 4, a dramatic change happens to the convergence. As shown in FIG. 3, the dynamical zeta function with cycles up to length 15 gives an escape rate with an error of 10^{-5} , while in the $A = 5$ case, the error is 10^{-15} . Moreover, the results obtained by the spectral determinant even lose the super-exponential convergence and exhibits



(a) the error of the escape rate computed with the dynamical zeta function



(b) the error of the escape rate computed with the spectral determinant

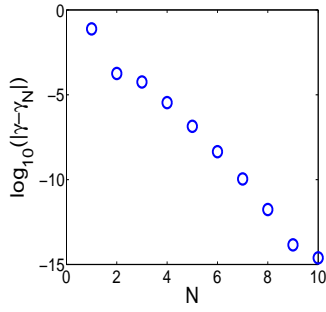
FIG. 1. The error of the escape rate for map $f(x) = 6x(1 - x)$ computed with (a) the dynamical zeta function and (b) the spectral determinant

only an exponential convergence. This phenomena implies that, in this special case, the spectral determinant may not be an entire function any more.

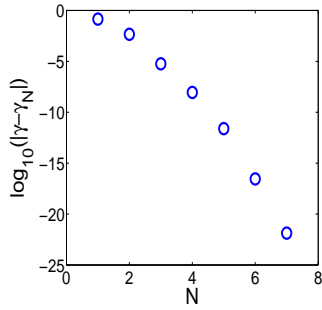
If we increase $A = 4$ to 4.001, we find that the convergence of the expansion improves dramatically, as depicted in Figure 4. When $A = 4.001$, the super-exponential convergence of the spectral determinant is restored.

The results above suggests that there must be something special for $A = 4$. An apparent property that makes the map of $A = 4$ different is that it has a critical point. To show that the existence of the critical point has a big influence on the convergence of cycle expansions, we use the dynamical zeta function to calculate the escape rate for maps with a higher-order critical point. One general type of maps is $f(x) = 1 - |2x - 1|^k$, $x \in [0, 1]$. [12]

In FIG. 5, as the order k becomes larger and larger, the top of the map becomes flatter and flat-

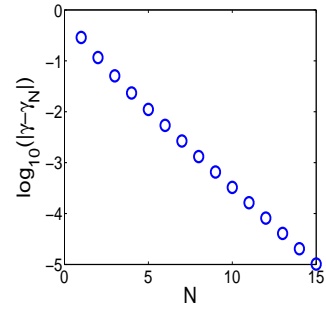


(a) the error of the escape rate computed with the dynamical zeta function

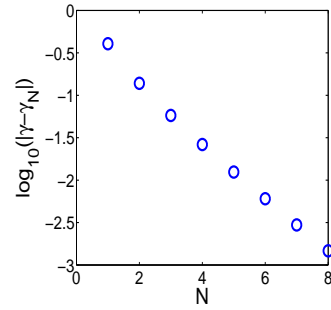


(b) the error of the escape rate computed with the spectral determinant

FIG. 2. The error of the escape rate for map $f(x) = 5x(1-x)$ computed with (a) the dynamical zeta function and (b) the spectral determinant



(a) the error of the escape rate computed with the dynamical zeta function



(b) the error of the escape rate computed with the spectral determinant

FIG. 3. The error of the escape rate for map $f(x) = 4x(1-x)$ computed with (a) the dynamical zeta function and (b) the spectral determinant

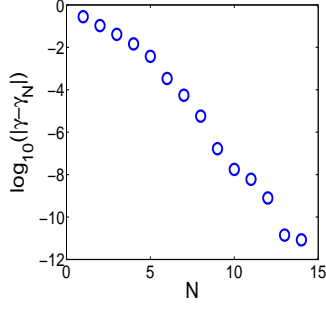
ter. The error of the escape rate obtained from the dynamical zeta function is displayed in FIG. 6 and FIG. 3(a), where we can see that the convergence is poorer for maps with a higher-order critical point. To know why the dynamical zeta function and the spectral determinant flaws for maps with critical points, we must have a clear understanding of the nature of the approximations when we apply a truncation to the dynamical zeta function.

D. The significance of the truncated dynamical zeta function

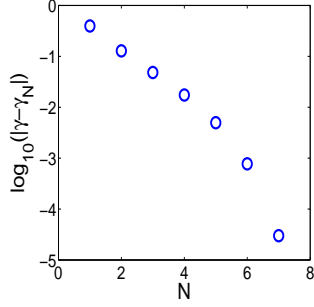
As we can not find all prime cycles, the number of which is infinite, we always apply a truncation to the dynamical zeta function. For example, if we truncate at the shortest cycles, we obtain the dynamical zeta function as $\frac{1}{\zeta} = 1 - t_0 - t_1$. The trun-

cated dynamical zeta function leaves out all the curvature corrections and is a rough approximation for the original map. Now, we ask one question: is there a linear map which has $\frac{1}{\zeta} = 1 - t_0 - t_1$ as its truncated first-order dynamical zeta function? A simple example is a piecewise linear map consisting of two pieces. The piecewise linear map is constructed in this way: firstly, find the fixed points of the map along with their derivatives at these points, then, draw line segments which pass the fixed points and are tangent to the graph of the map. If we want to construct a piecewise linear map which has a dynamical zeta function similar to that of the original map up to order N , we need the positions and derivatives of all the periodic points of period not larger than N . FIG. 7 displays a piecewise linear map for the truncation up to length two, while the original map is $f(x) = 4x(1-x)$.

The dynamical averages obtained by the N th-



(a) the error of the escape rate computed with the dynamical zeta function



(b) the error of the escape rate computed with the spectral determinant

FIG. 4. The error of the escape rate for map $f(x) = 4.001x(1-x)$ computed with (a) the dynamical zeta function and (b) the spectral determinant

order truncation is nearly identical to the one computed with the corresponding piecewise linear map. For the piecewise linear map, the curvature corrections with order larger than N are nearly zero due to its linearity, and therefore, we regard the piecewise linear map as a prototyped geometric model of the N th-order truncated dynamical zeta function. The dynamical averages computed with the N th-order truncated dynamical zeta function are very close to those given by the piecewise linear map. So, how well the piecewise linear map approximates the original map determines the computation accuracy of the truncation.

We know that the average obtained from the dynamical zeta function is equivalent to a phase space average $\langle a \rangle = \int_{\mathcal{M}} dx \rho(x) a(x)$, where $\rho(x)$ is the natural measure. For example, for the tent map, the natural measure is uniform everywhere. However, for the map with critical points, the natural mea-

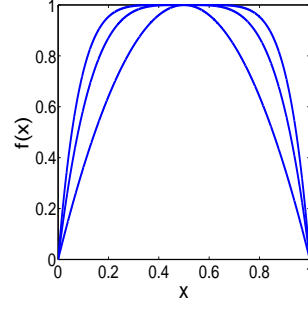
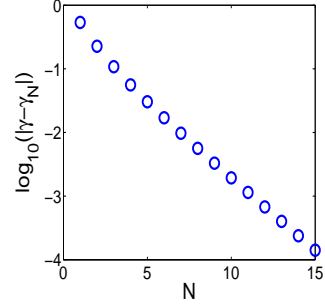
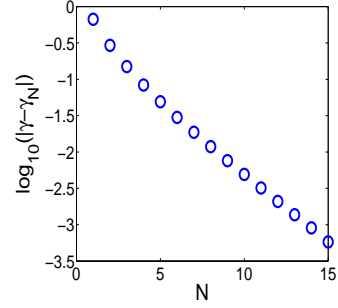


FIG. 5. $f(x) = 1 - (2x - 1)^k$, $k = 2, 4, 6$



(a) the error of the escape rate for map $f(x) = 1 - (2x - 1)^4$



(b) the error of the escape rate for map $f(x) = 1 - (2x - 1)^6$

FIG. 6. The error of the escape rate for maps with a higher-order critical point computed with the dynamical zeta function

sure has singularities as portrayed in FIG. 8.

It's just these singularities that lead to the slow convergence in a cycle expansion, because the piecewise linear map obtained from the truncated dynamical zeta function can not represent well the natu-

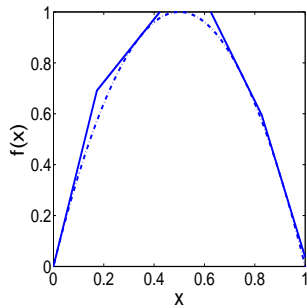


FIG. 7. A piecewise linear map approximation of the map $f(x) = 4x(1-x)$

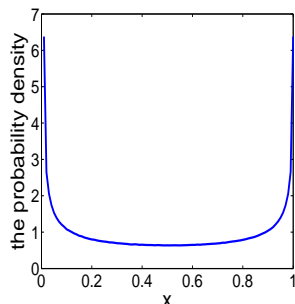


FIG. 8. The natural measure of map $f(x) = 4x(1-x)$

ral measure with singularities. Though the natural measure of the piecewise linear map gets closer and closer to that of the original map with increasing truncation length, it fails near the singularity. As a result, the average obtained from the piecewise linear map, or equivalently, from the truncated dynamical zeta function does not converge as fast as in the uniformly hyperbolic case.

E. Accelerating convergence in the presence of the critical point

We find that the singularity in the natural measure causes the slow convergence of the dynamical zeta function. A natural cure of this trouble is to clear out the singularity by a coordinate transformation, which results in a new map conjugate to the original map but without a singularity in the natural measure. We will show that we can accelerate the convergence with the help of the conjugate

map.

1. Clear out the singularities

For maps with a critical point, such as $f(x) = 1 - |2x-1|^k$, $k = 2, 4, 6, \dots$, the probability distribution has an algebraic form in the neighborhood of the singularity, for example

$$\rho(x) \sim \frac{1}{x^{\frac{k-1}{k}}} \text{ near } x = 0, \quad (12)$$

where k is the order of the critical point. For example, the natural measure of the map $f(x) = 1 - (2x-1)^2$ has two singular points: 0 and 1, with the probability distribution $\rho(x) \sim \frac{1}{\sqrt{x}}$ near $x = 0$ and $\rho(x) \sim \frac{1}{\sqrt{1-x}}$ near $x = 1$.

We need a coordinate transformation that stretches the coordinate axis around the singularity in order to remove it. We are able to construct a transformation $h : \mathcal{M} \rightarrow \mathcal{M}$ of the form $h(x) \propto |x - x_0|^{1/k}$ in the neighborhood of the singularity $x = x_0$ to achieve this goal. For the map $f(x) = 1 - (2x-1)^2 = 4x(1-x)$, $[0, 1] \rightarrow [0, 1]$, an appropriate transformation is $h(x) = \frac{2}{\pi} \arcsin \sqrt{x}$, which you can see has the desired form in the neighborhood of 0 and 1.

With the coordinate transformation, the original map is changed to its conjugate map. Denoting the original map by $f(x)$ and the conjugate by $g(x')$, we have the relationship that $f = h^{-1} \circ g \circ h$, or equivalently, $g = h \circ f \circ h^{-1}$. The map $f(x) = 1 - (2x-1)^2 = 4x(1-x)$ and its conjugate are displayed in FIG. 9.

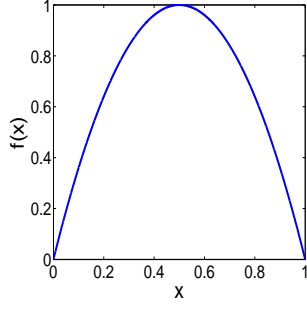
The conjugate map has no critical point any more, and the natural measure produced by the two maps are displayed in FIG. 10, in which we can see that the natural measure of the conjugate map has no singularity any more.

2. The conjugate dynamical zeta function

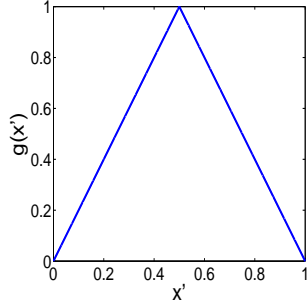
In an ergodic system, the dynamical average $\langle a \rangle$ can be obtained through the time averaging, as well as an average on the natural measure. Through the time averaging, the average is computed as

$$\langle a \rangle = \frac{1}{N} \sum_{i=0}^N a(x_i), \quad (13)$$

where $x_0 \rightarrow x_1 \rightarrow \dots \rightarrow x_i \rightarrow \dots \rightarrow x_N$ is an itinerary generated by the map and N is a number large enough.



(a) $f(x) = 4x(1-x)$



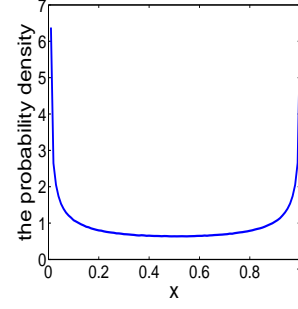
(b) the conjugate map

FIG. 9. (a) map $f(x) = 4x(1-x)$ and (b) its conjugate map

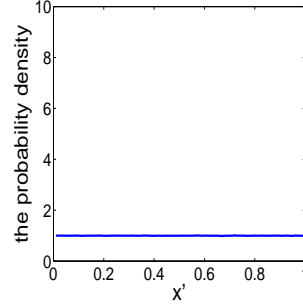
An ergodic map $f : X \rightarrow X$ and its conjugate $g = h \circ f \circ h^{-1} : X' \rightarrow X'$ is related by the conjugacy $h : X \rightarrow X'$. If we have the iteration $f(x_i) = x_{i+1}$, under the conjugation $h(x_i) = x'_i$, $g(x'_i) = x'_{i+1}$, which is to say, a trajectory $\{x_i\}$ for the map $f(x)$ transforms into one trajectory $\{x'_i\}$ for the map $g(x')$. In particular, the cycle for the map $f(x)$ is a cycle for the map $g(x')$. If the conjugacy h is piecewise smooth, a typical trajectory has identical weight in both coordinates, which suggests that the dynamical average can be obtained with the help of the map $g(x')$,

$$\langle a \rangle_f = \frac{1}{N} \sum_{i=1}^N a(x_i) = \frac{1}{N} \sum_{i=1}^N a(h^{-1}(x'_i)) = \langle a \circ h^{-1} \rangle_g. \quad (14)$$

This means that we can compute the average $\langle a \rangle$ under the map $f(x)$ through the average $\langle a \circ h^{-1} \rangle$ under the map $g(x')$. Based on the discussion above, we introduce a concept: the conjugate dynamical zeta function.



(a) the natural measure of map $f(x) = 4x(1-x)$



(b) the natural measure of the conjugate map

FIG. 10. the natural measure (a) of map $f(x) = 4x(1-x)$ and (b) of its conjugate map

Definition 1. Suppose that map $f(x)$ and $g(x')$ are conjugate, with $f = h^{-1} \circ g \circ h$. The observable a for map $f(x)$ has a correspondent $a \circ h^{-1}$ for map $g(x')$. The dynamical zeta function $\frac{1}{\zeta}$ for $f(x)$ and a and $\frac{1}{\zeta'}$ for $g(x')$ and $a \circ h^{-1}$ are said to be conjugate. We call h the conjugacy between $\frac{1}{\zeta}$ and $\frac{1}{\zeta'}$.

It's obvious that the dynamical averages obtained by $\frac{1}{\zeta}$ and $\frac{1}{\zeta'}$ are the same, since $\langle a \rangle_f = \langle a \circ h^{-1} \rangle_g$. The exact form for $\frac{1}{\zeta}$ and $\frac{1}{\zeta'}$ is respectively

$$\begin{aligned} \frac{1}{\zeta} &= \prod_p (1 - t_p), \quad t_p = z^{n_p} \frac{e^{\beta A_p}}{|\Lambda_p|} \\ \frac{1}{\zeta'} &= \prod_p (1 - t'_p), \quad t'_p = z^{n_p} \frac{e^{\beta A'_p}}{|\Lambda'_p|}, \end{aligned} \quad (15)$$

where $A'_p = \sum_{i=1}^{n_p} a(h^{-1}(x'_i)) = \sum_{i=1}^{n_p} a(x_i) = A_p$. So, A_p is the same as the corresponding A'_p , no matter if h is diffeomorphic or not. If h is diffeomorphic, the cycle stability eigenvalue Λ_p is also the same as the corresponding Λ'_p . Thus, we obtain $\frac{1}{\zeta} = \frac{1}{\zeta'}$. However, when h is not diffeomorphic, the cycle stability eigenvalue may be changed and so does the

dynamical zeta function, i.e., $\frac{1}{\zeta} \neq \frac{1}{\zeta'}$. This happens when we use the coordinate transformation to clear out the singularities in the natural measure.

3. The changes of the conjugate dynamical zeta function

We mentioned in Section III E 1 that to clear out the singularities, we need a coordinate transformation $h \propto |x - x_0|^{1/k}$ near the singular point x_0 . The derivative of h has the form: $\frac{dh}{dx} \propto \frac{1}{|x - x_0|^{1 - \frac{1}{k}}}$. So, the dh/dx has a singularity at $x = x_0$. Thus, the conjugacy h is not diffeomorphic at the singular point. If one periodic point happens to be singular, the stability eigenvalue of the periodic orbit will be changed.

For example, for the map $f(x) = 1 - |2x - 1|^k$, the fixed point $\bar{0}$ is a singular point of natural measure. So, the stability Λ_0 for $\bar{0}$ is changed to $\Lambda_0^{1/k}$, as shown below.

In the neighborhood of the fixed point $\bar{0}$, the asymptotic form for f and h is $f \sim \Lambda_0 x$, $x > 0$ and $h \sim ax^{\frac{1}{k}}$, where $a > 0$ is a coefficient. We have

$$\begin{aligned} g(x') &= h \circ f \circ h^{-1}(x') \\ &\sim h \circ f(x^k/a^k) \sim h(\Lambda_0 x^k/a^k) \sim \Lambda_0^{1/k} x' \end{aligned} \quad (16)$$

Hence stability Λ_0 of $\bar{0}$ for the conjugate map g is changed to $\Lambda_0^{1/k}$.

So, in this situation, $\frac{1}{\zeta'} \neq \frac{1}{\zeta}$. Nevertheless, for the map $f(x) = 1 - |2x - 1|^k$, if the conjugacy is diffeomorphic except at $x = 0, 1$, the only difference in $\frac{1}{\zeta'}$ is $\Lambda_0' = \Lambda_0^{1/k}$, compared to $\frac{1}{\zeta}$. As the conjugate dynamical zeta function $\frac{1}{\zeta'}$ is computed for map $g(x')$ whose natural measure has no singularity, the convergence for $\frac{1}{\zeta'}$ is much improved than $\frac{1}{\zeta}$. Note that the exact functional form of the conjugacy is not essential as long as it has the right asymptotic forms near the singular point.

F. Several examples

We proved that dynamical averages in a map can be computed with its conjugate map. For a map with critical points, we should find an appropriate coordinate transformation to clear out singularities in the natural measure. The conjugate map behaves much better in the sense that the influence of critical points is cleared out and the convergence of the conjugate dynamical zeta function is accelerated. More-

over, we do not have to know the exact functional form of the coordinate transformation. What we do is change stability eigenvalues of specific cycles supported on the singularities in the original map and hence transform the dynamical zeta function to its conjugate.

We apply our method to several examples. All these maps have critical points and therefore, produce natural measure with singularities.

1. The logistic map

The logistic map $f(x) = 4x(1 - x)$, $x \in [0, 1]$ has a critical point of order two. Its natural measure is singular at two points: $x = 0$ and $x = 1$. Under the transformation $h = \frac{2}{\pi} \arcsin \sqrt{x}$, the singularities in its natural measure are cleared out, as shown in FIG. 10. Also, the conjugate map $g(x') = h \circ f(x) \circ h^{-1}$ has no critical point any more, as depicted in FIG. 9.

In the map $g(x')$, the stability eigenvalue of the fixed point $\bar{0}$ is $\Lambda_0^{1/2} = 2$ where $\Lambda_0 = 4$ is the stability eigenvalue of the corresponding point in the logistic map, with stability eigenvalues of all the other orbits remaining the same.

The logistic map has an interesting property: the eigenvalue for any prime cycle except $\bar{0}$ has an absolute value of 2^n , where n is the length of the cycle. However, the eigenvalue of $\bar{0}$ is $\Lambda_0 = 4$. After the coordinate transformation, the absolute value of the eigenvalue of any prime cycle of length n is 2^n , returning to the tent map case.

Thanks to this identity, the conjugate dynamical zeta function under conjugation h is just

$$\frac{1}{\zeta'} = 1 - z, \quad (17)$$

which is the same dynamical zeta function of the tent map. So, the escape rate of the logistic map is exactly 0.

Similar to the conjugate dynamical zeta function, we can write out the conjugate spectral determinant, only with the change $\Lambda_0' = \Lambda_0^{1/2} = 2$. For the conjugate spectral determinant, the error of escape rate decreases super-exponentially, as shown in FIG. 11. However, if we apply the spectral determinant directly to the logistic map, the error of escape rate decreases exponentially with the truncation length N , as shown in FIG. 3(b). So, by an appropriate coordinate transformation, we bring the super-exponential convergence back, which signals that the influence of critical points is cleared out.

Certainly, the logistic map here is very special since it is exactly conjugate to a tent map [24]. To show the general applicability of the technique, in the following, we apply the method to several other maps for which no smooth conjugacy to the piecewise linear map is known.

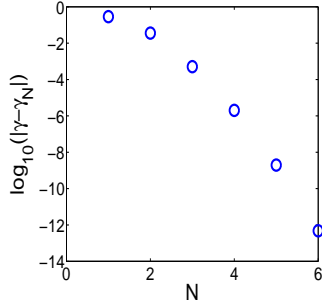
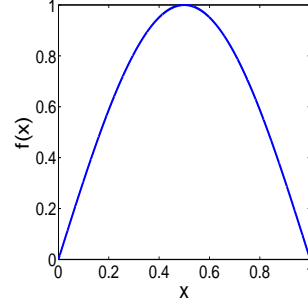


FIG. 11. The error of the escape rate for the logistic map computed with the conjugate spectral determinant

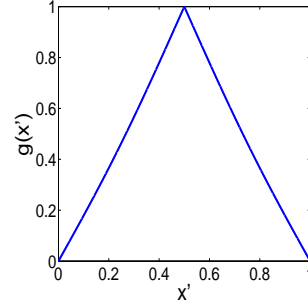
2. Map $f(x) = \sin(\pi x)$

The map $f(x) = \sin(\pi x)$, $x \in [0, 1]$ has a critical point of order two. Its natural measure has two singular points: $x = 0$ and $x = 1$. The asymptotic form of its natural measure near the singularity is $\rho \sim \frac{1}{\sqrt{x}}$ near $x = 0$ and $\rho \sim \frac{1}{\sqrt{1-x}}$ near $x = 1$. All these properties are similar to those of the logistic map. Under the coordinate transformation $h = \frac{2}{\pi} \arcsin \sqrt{x}$, the singularities of the natural measure are removed, and we obtain the conjugate map $g(x') = h \circ f(x) \circ h^{-1}$. FIG. 12 portrays the map $f(x)$ and $g(x')$ where the critical point that exists in $f(x)$ disappears in the map $g(x')$. FIG. 13 displays the natural measure produced by the map $f(x)$ and $g(x')$ respectively where the singularity at $x = 0, 1$ vanishes by $g(x')$

For the conjugate map g , the stability eigenvalue of fixed point $\bar{0}$ is changed from $\Lambda_0 = \pi$ to $\Lambda_0 = \pi^{1/2}$, while the eigenvalue of any other orbit doesn't change. We use the dynamical zeta function and its conjugate to calculate the escape rate, $\langle x \rangle$, $\langle x^2 \rangle$, $\langle x^3 \rangle$ of the map $f(x) = \sin \pi x$. The results are shown in TABLE II, with a cutoff of cycle length 10. Also included are the results obtained by direct time averaging, with 10^7 iterations. From TABLE II we can see that the results obtained from the conjugate dynamical zeta function are by far the



(a) map $f(x) = \sin(\pi x)$



(b) the conjugate map $g(x')$

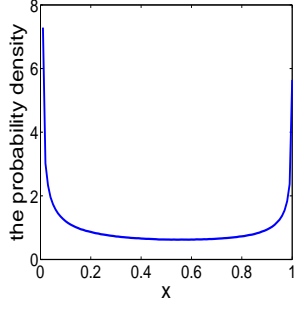
FIG. 12. The graph of (a) $f(x) = \sin(\pi x)$ and (b) its conjugate map $g(x')$

most accurate.

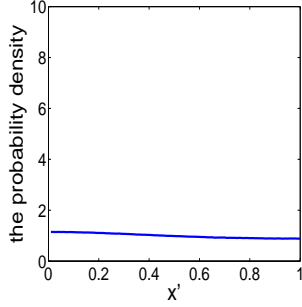
	the dynamical zeta function	the conjugate dynamical zeta function	time averaging
escape rate	9×10^{-4}	-3×10^{-11}	
$\langle x \rangle$	0.47	0.46796294	0.468
$\langle x^2 \rangle$	0.34	0.34397492	0.344
$\langle x^3 \rangle$	0.28	0.283947287	0.284

TABLE II. The escape rate, $\langle x \rangle$, $\langle x^2 \rangle$, $\langle x^3 \rangle$ for map $f = \sin(\pi x)$ obtained by three different ways

FIG. 14 displays errors in the averages obtained by the dynamical zeta function for $f(x) = \sin(\pi x)$ and its conjugate with different truncation length. Although all the errors seem to decrease exponentially, the results from the conjugate dynamical zeta function decay much faster, indicating a great improvement of the convergence.



(a) the natural measure of $f(x) = \sin(\pi x)$



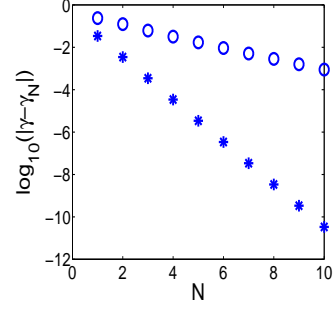
(b) the natural measure of the conjugate map $g(x')$

FIG. 13. the natural measure of (a) $f(x) = \sin(\pi x)$ and (b) its conjugate map $g(x')$

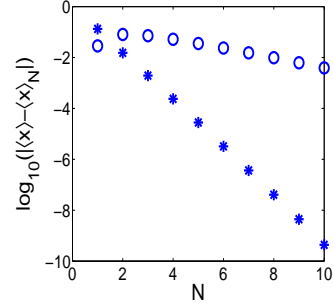
3. Map $f(x) = 1 - (2x - 1)^4$

The map $f(x) = 1 - (2x - 1)^4$ has a critical point of order four, with measure singularities at $x = 0$ and $x = 1$. The asymptotic form of the natural measure near the singularity is $\rho \sim \frac{1}{x^{3/4}}$ near $x = 0$ and $\rho \sim \frac{1}{(1-x)^{3/4}}$ near $x = 1$ as shown in FIG. 16(a). To remove the singularities, an appropriate coordinate transformation h is $h = 1 - \frac{\arccos(1-2\sqrt{1-\sqrt{x}})}{\pi}$, which has an asymptotic form $h \propto x^{1/4}$ near $x = 0$ and $h \propto (1-x)^{1/4}$ near $x = 1$. Thus, we obtain the conjugate map $g(x') = h \circ f(x) \circ h^{-1}$. The map $f(x)$ and its conjugate $g(x')$ are depicted in FIG. 15. Although $f(x)$ has a very flat top, the peak of $g(x')$ is acute. As a result, the natural measure of the map $g(x')$ has no singularity, displayed in FIG. 16(b).

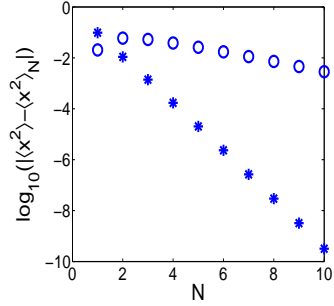
The stability eigenvalue of $\bar{0}$ of the conjugate map is $\Lambda'_0 = \Lambda_0^{1/4} = 8^{1/4}$. The convergence of the dynamical zeta function for $f(x) = 1 - (2x - 1)^4$ is



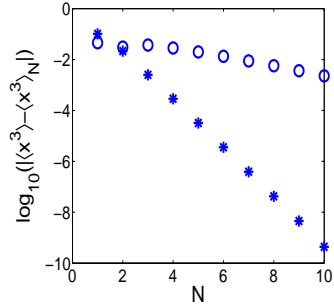
(a) the error of escape rate



(b) the error of $\langle x \rangle$

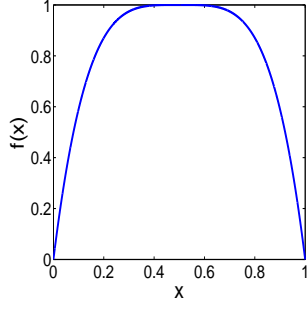


(c) the error of $\langle x^2 \rangle$

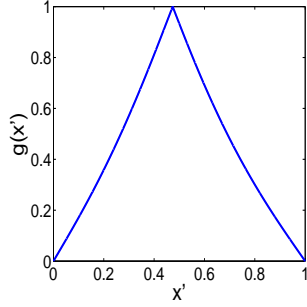


(d) the error of $\langle x^3 \rangle$

11 FIG. 14. the error of the escape rate, $\langle x \rangle$, $\langle x^2 \rangle$, $\langle x^3 \rangle$ obtained by the dynamical zeta function for $f = \sin(\pi x)$ and its conjugate dynamical zeta function



(a) the map $f(x) = 1 - (2x - 1)^4$



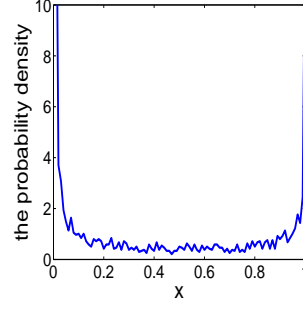
(b) the conjugate map

FIG. 15. The graph of (a) the map $f(x) = 1 - (2x - 1)^4$ and (b) its conjugate map

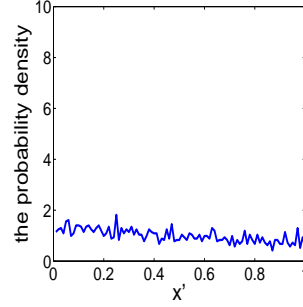
even poorer than the logistic map. However, the conjugate dynamical zeta function continues to give a much accelerated convergence. The escape rate, $\langle x \rangle, \langle x^2 \rangle, \langle x^3 \rangle$ obtained by the two different ways are shown in TABLE III, with a truncation length 10. It is worth mentioning that the direct time averaging becomes very unreliable in the current case. FIG. 17 plots the errors in these averages with different truncation length. We can see that the conjugate dynamical zeta function converges much faster.

	the dynamical zeta function	the conjugate dynamical zeta function
escape rate	2×10^{-3}	-2×10^{-9}
$\langle x \rangle$	0.45	0.4475860
$\langle x^2 \rangle$	0.37	0.3601271
$\langle x^3 \rangle$	0.32	0.31801265

TABLE III. The escape rate, $\langle x \rangle, \langle x^2 \rangle, \langle x^3 \rangle$ for map $f(x) = 1 - (2x - 1)^4$ obtained by two different ways



(a) the natural measure of $f(x) = 1 - (2x - 1)^4$



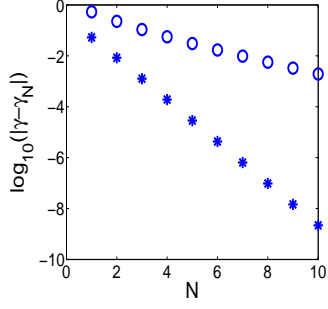
(b) the natural measure of the conjugate map

FIG. 16. The natural measure of (a) $f(x) = 1 - (2x - 1)^4$ and (b) its conjugate map

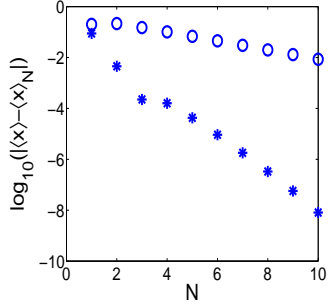
4. Map $f(x) = 1 - (2x - 1)^6$

Map $f(x) = 1 - (2x - 1)^6$ has a critical point of order six, and therefore causes an even worse convergence for the dynamical zeta function, as shown in FIG. 6(b). The coordinate transformation we use is $h = 1 - \frac{\arccos(1 - 2(1 - x^{\frac{1}{3}})^{\frac{1}{3}})}{\pi}$, and the conjugate map $g(x') = h \circ f(x) \circ h^{-1}$ has no critical point any more. Thus, the singularities of natural measure are also removed. FIG. 18 shows the graph of map $f(x)$ and $g(x')$. The natural measure of map $f(x)$ and $g(x')$ is depicted in FIG. 19, obtained with 10^8 iterations in this case. We can see that both the natural measures fluctuates, which implies that the time averages based on iterations can't reach a high accuracy for this map.

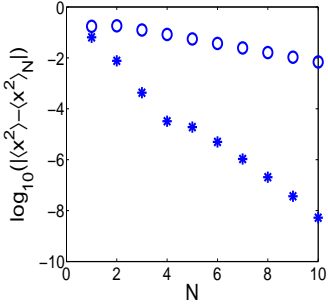
For the conjugate dynamical zeta function, the only difference from the original dynamical zeta function is that, the stability eigenvalue of $\bar{0}$ is changed to $\Lambda'_0 = \Lambda_0^{\frac{1}{6}} = 12^{\frac{1}{6}}$. The values of aver-



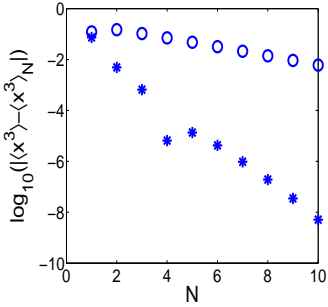
(a) the error of escape rate



(b) the error of $\langle x \rangle$

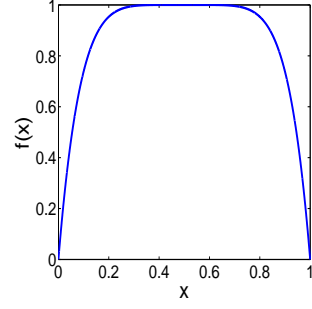


(c) the error of $\langle x^2 \rangle$

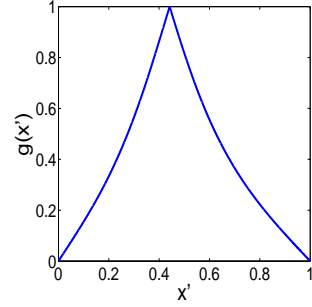


(d) the error of $\langle x^3 \rangle$

FIG. 17. The error of the escape rate, $\langle x \rangle$, $\langle x^2 \rangle$, $\langle x^3 \rangle$ obtained by the dynamical zeta function for $f(x) = 1 - (2x - 1)^4$ and its conjugate dynamical zeta function



(a) the map $f(x) = 1 - (2x - 1)^6$



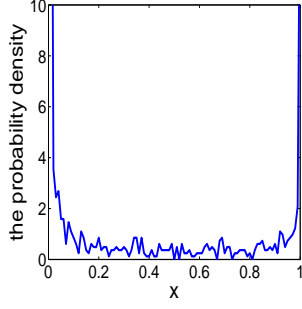
(b) the conjugate map

FIG. 18. The graph of (a) the map $f(x) = 1 - (2x - 1)^6$ and (b) its conjugate map $g(x')$

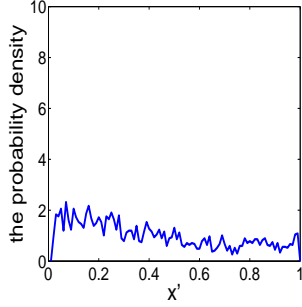
ages obtained by the two dynamical zeta functions, with a truncation length 10, are listed in TABLE IV, while the dependence of the computational errors on the truncation length is portrayed in FIG. 20. We can see that the conjugate dynamical zeta function converges much faster than the original zeta function, which provides evidence that clearing out the singularity in natural measure helps accelerate the convergence.

	the dynamical zeta function	the conjugate dynamical zeta function
escape rate	5×10^{-3}	-2×10^{-7}
$\langle x \rangle$	0.4	0.40232
$\langle x^2 \rangle$	0.34	0.332921
$\langle x^3 \rangle$	0.31	0.30027

TABLE IV. The escape rate, $\langle x \rangle$, $\langle x^2 \rangle$, $\langle x^3 \rangle$ for the map $f(x) = 1 - (2x - 1)^6$ obtained by two different ways



(a) the natural measure of the map $f(x) = 1 - (2x - 1)^6$

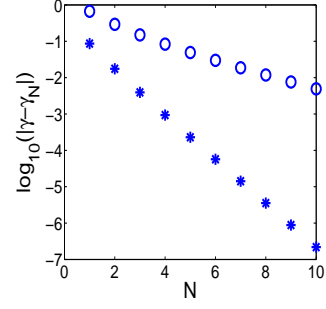


(b) the natural measure of the conjugate map $g(x')$

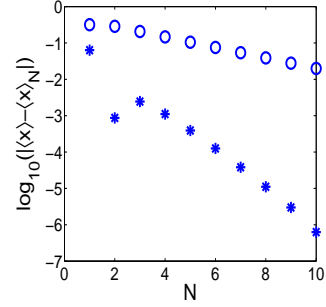
FIG. 19. The natural measure of the map $f(x) = 1 - (2x - 1)^6$ and its conjugate map $g(x')$

5. Map with three measure singularities

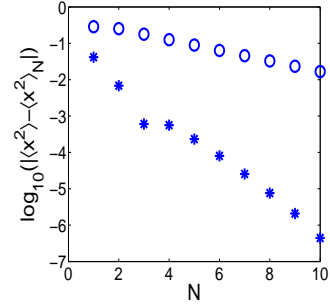
The maps we have studied so far all have two measure singularities: $x = 0$ and $x = 1$. In this section, we turn to a map with three measure singularities, the graph of which is shown in FIG. 21(a). The exact functional form of the map is $f = \sin(\frac{\pi}{a}(1 - x))$, where $a = 1.3156445888\dots$. It has a critical point of order two, and has a nice property: $f(0) = x_f$, where x_f is the unique fixed point of the map. The natural measure of f has three singularities: $x = 0, x_f, 1$. The asymptotic form of the natural measure near the singularity is $\rho \sim \frac{1}{\sqrt{x}}$ near $x = 0$, $\rho \sim \frac{1}{\sqrt{|x - x_f|}}$ near $x = x_f$ and $\rho \sim \frac{1}{\sqrt{1 - x}}$ near $x = 1$, as shown in FIG. 22(a). To clear out the singularities, we use one coordinate transformation h depicted in FIG. 23, which stretches the coordinate around the singularities. The conjugate map $g(x')$ is nearly a piecewise linear map, as shown in FIG. 21(b). The natural measure of the map $g(x')$ is depicted in FIG. 22(b),



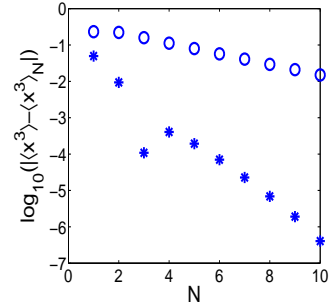
(a) the error of escape rate



(b) the error of $\langle x \rangle$



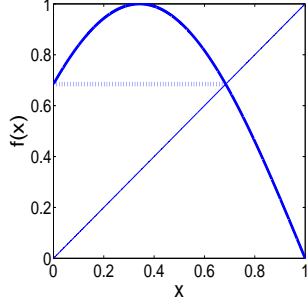
(c) the error of $\langle x^2 \rangle$



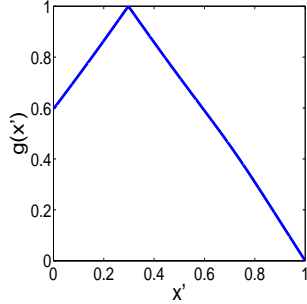
(d) the error of $\langle x^3 \rangle$

14 FIG. 20. The error of the escape rate, $\langle x \rangle, \langle x^2 \rangle, \langle x^3 \rangle$ obtained by the dynamical zeta function for $f(x) = 1 - (2x - 1)^6$ and its conjugate dynamical zeta function

which has no singularity any more.



(a)The map with three measure singularities



(b)The conjugate map

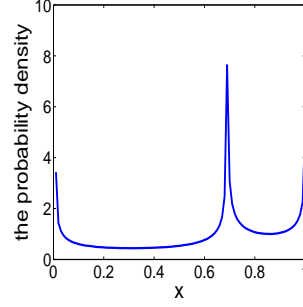
FIG. 21. The graph of (a) the map with three measure singularities and (b) its conjugate map

For the conjugate dynamical zeta function, the stability of \bar{x}_f should be changed to $|\Lambda_{x_f}|' = |\Lambda_{x_f}|^{\frac{1}{2}}$. Again, we use the original and the conjugate dynamical zeta function to calculate averages. The results are listed in TABLE V, with a cutoff of cycle length 20. The errors in the computation are plotted in FIG. 24.

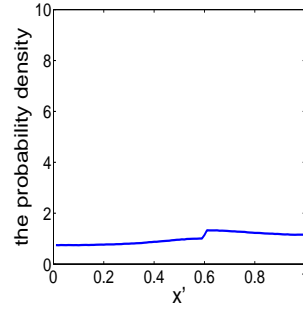
By clearing out the singularities in the natural measure, the convergence is accelerated a lot. So, in this case, the conjugate dynamical zeta function is still an effective way to obtain averages with high accuracy.

6. Map with measure singularities on a period-2 orbit

The conjugation method may be applied to systems with measure singularity on longer orbits. As an example, we study a map with measure singularities on a period-2 orbit. The functional form of the



(a)The natural measure of the map with measure three singularities



(b)The natural measure of the conjugate map

FIG. 22. The natural measure of (a) the map with three measure singularities and (b) its conjugate map

	the dynamical zeta function	the conjugate dynamical zeta function
escape rate	5×10^{-4}	-1×10^{-10}
$\langle x \rangle$	0.601	0.60189561
$\langle x^2 \rangle$	0.453	0.453165976
$\langle x^3 \rangle$	0.365	0.36466994

TABLE V. The averages for the map with three measure singularities by two different ways

map is still $f(x) = \sin(\frac{\pi}{a}(1-x))$, but with a different value $a = 1.10263451544766\dots$. FIG. 25(a) portrays the graph of the map. For this map, $f(0) = x_a$, $f^2(0) = x_b$, where x_a and x_b make a period-2 orbit. The natural measure of the map is shown in FIG. 26(a), which has four singularities: $x = 0, x_a, x_b, 1$. The appropriate conjugacy h is plotted in FIG. 27, which stretches the coordinate around the four singularities. The conjugate map $g(x')$ and its natural measure is plotted in FIG. 25(b)

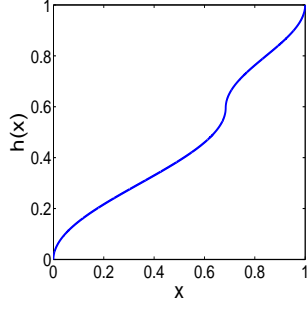


FIG. 23. The conjugacy h for the map with three measure singularities

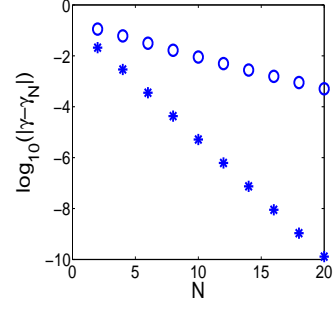
and FIG. 26(b) respectively. For the map $g(x')$, the singularities has been removed—the situation that we have encountered many times.

We change the eigenvalue of the period-2 orbit and obtain the conjugate dynamical zeta function—just as what we have done many times. Next, we use the conjugate dynamical zeta function to calculate the escape rate. The results are amazing. FIG. 28 shows the error in the escape rate by the original and the conjugate dynamical zeta function. In general, the results obtained by the conjugate dynamical zeta function converge exponentially and uniformly faster than the results obtained by the original dynamical zeta function. However, it's not the case here. The conjugate dynamical zeta function doesn't accelerate the convergence as effectively as before. So, why the convergence for the conjugate dynamical zeta function is not so good even if we have removed the measure singularities?

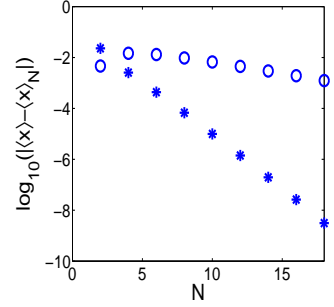
If we look at the FIG. 25(b), the graph of the conjugate map, in detail, we could find one point where the derivative is infinite. It's just this point that causes the slow convergence. We regard this infinite slope map as “super-hyperbolic”. The super-hyperbolic map doesn't accelerate but slows down the convergence. To illustrate this point, we use the dynamical zeta function to calculate the escape rate of a super-hyperbolic map f ,

$$f = \begin{cases} 2x & x \in [0, 1/2] \\ \sqrt{2-2x} & x \in [1/2, 1] \end{cases} \quad (18)$$

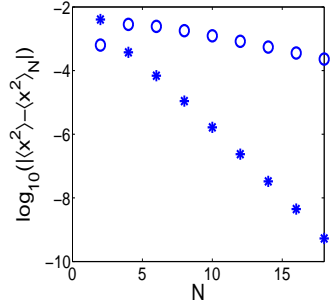
where $f'(1) = \infty$. We compare the results of this map and the logistic map, which are displayed in FIG. 29. Both results are computed with the original dynamical zeta function. We can see that the speeds of convergence are similar for these two maps.



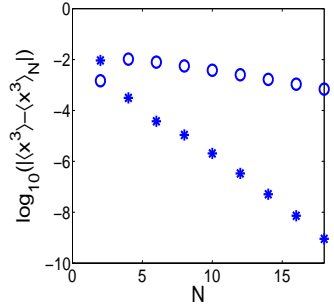
(a) the error of escape rate



(b) the error of $\langle x \rangle$

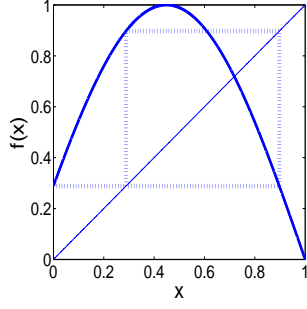


(c) the error of $\langle x^2 \rangle$

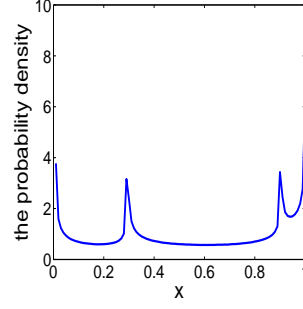


(d) the error of $\langle x^3 \rangle$

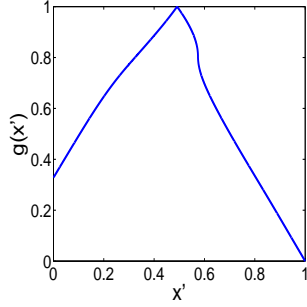
16 FIG. 24. The error of the escape rate, $\langle x \rangle$, $\langle x^2 \rangle$, $\langle x^3 \rangle$ obtained by the dynamical zeta function for the map with three measure singularities and its conjugate dynamical zeta function



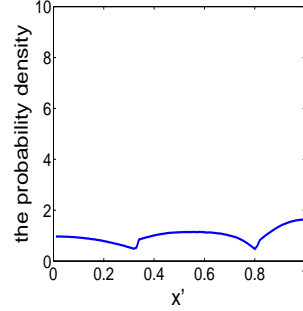
(a)The map with measure singularities on a period-2 orbit



(a)The natural measure of map f



(b)The conjugate map



(b)The natural measure of the conjugate map

FIG. 25. (a) The map with measure singularities on a period-2 orbit and (b) its conjugate map

FIG. 26. The natural measure of (a) the map with measure singularities on a period-2 orbit and (b) its conjugate map

So, the super-hyperbolicity is harmful to the convergence, just like the non-hyperbolicity. To understand this, we recall the fact that the average obtained by the truncated dynamical zeta function is nearly identical to the one computed with the corresponding piecewise linear map. So, if the piecewise linear map can approximate the original map very well, the average obtained would be quite precise. However, for the super-hyperbolic map, there exists a point whose derivative is infinite, which means that the value of the map changes dramatically near that point. So, we need a lot of cycle points near that point if we want to get a fair approximation. Thus, the slow convergence of the super-hyperbolic map is expected.

Based on the discussion above, we can see that the singularity of natural measure is not the only factor which influences the convergence of the dynamical zeta function. For the map with measure singularities on a period-2 orbit, clearing out the measure singularities doesn't improve the convergence much.

In fact, the direct and essential factor to determine the convergence of the dynamical zeta function is the cancellation of prime cycles and pseudo-cycles. For the super-hyperbolic case, the cancellation is not strong even if the measure singularities do not exist. So, in the super-hyperbolic case, how to incur further cancellation remains a challenging problem.

IV. CONCLUSION

The central idea of this paper is that by clearing out the singularities in the natural measure we may accelerate the convergence of cycle expansions. Maps with critical points produce natural measures with singularities and show bad convergence in the expansion calculation. By appropriate coordinate transformation, the resulted conjugate maps produce no singularity in its natural measure. To calculate dynamical averages, we use the conjugate spec-

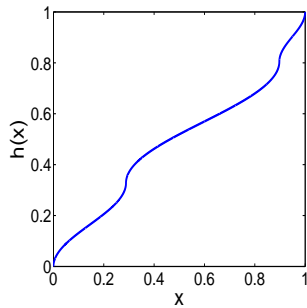


FIG. 27. The conjugacy h for the map with measure singularities on a period-2 orbit

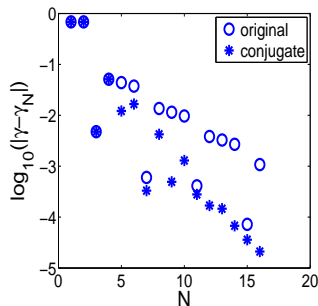


FIG. 28. The error of the escape rate by the original and the conjugate dynamical zeta function for the map with measure singularities on a period-2 orbit

tral function, the cycle expansion of which is greatly accelerated due to the removal of the singularities. Essentially, the method locates the leading poles of the spectral function by observing the singularity in the natural measure and removes them by coordinate transformation.

We test our method on several maps, *i.e.*, $f(x) = 1 - |2x - 1|^k$, $k = 2, 4, 6$, $f(x) = \sin(\pi x)$ which have only one critical point and complete binary dynamics, and the map which have three measure singularities. For these maps, the conjugate dynamical zeta function converges much faster than the origi-

nal one. Also, the conjugate spectral determinant restores the super-exponential convergence. However, when we treat the map with measure singularities on a period-two orbit, we find that the conjugate dynamical zeta function does not converge as fast as expected. Analysis shows that the super-hyperbolicity of the conjugate map leads to this slowing-down.

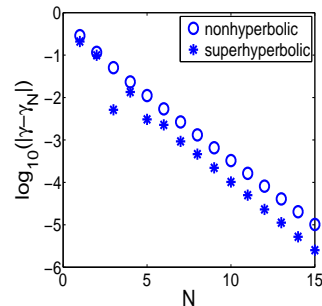


FIG. 29. The error of the escape rate for the super-hyperbolic map and the non-hyperbolic map

Further study is needed to eliminate this trouble.

In this paper, we use one-dimensional maps as examples to demonstrate our accelerating schemes. How to generalize it to higher dimensions or to flows requires further investigation. Even in the 1-d case, we can only treat maps with symbolic dynamics being subshift of finite type. If the genealogy sequence of the critical point is not essentially periodic, there may exist a natural boundary in the complex plane for the dynamical zeta function on which singular points are dense. In this case, the natural measure is singular on a dense and countable set [10]. It seems not possible to expand the radius of expansion by analytic continuation. Novel technique has to be invented to treat this problem.

ACKNOWLEDGEMENTS

This research is supported by National Natural Science Foundation of China (Grant No. 10975081).

[1] R. Artuso, E. Aurell, and P. Cvitanović. Recycling of strange sets: I. cycle expansions. *Nonlinearity*, 3:325, 1990.

[2] R. Artuso, E. Aurell, and P. Cvitanović. Recycling of strange sets: II. applications. *Nonlinearity*, 3:361, 1990.

- [3] R. Artuso, P. Cvitanović, and G. Tanner. Cycle expansions for intermittent maps. *Proc. Theor. Phys. Supp.*, 150:1–21, 2003.
- [4] E. Aurell. Convergence of dynamical zeta functions. *J. Stat. Phys.*, 58:967, 1990.
- [5] P. Cvitanović. *Universality in Chaos*. Adam Hilger, Bristol, 1989. Second Edition.
- [6] P. Cvitanović. Periodic orbits as the skeleton of classical and quantum chaos. *Physica D*, 51:138, 1991.
- [7] P. Cvitanović, R. Artuso, R. Mainieri, G. Tanner, and G. Vattay. *Chaos: Classical and Quantum*. Niels Bohr Institute, Copenhagen, 2005. ChaosBook.org.
- [8] P. Cvitanović, K. Hansen, J. Rolf, and G. Vattay. Beyond the periodic orbit theory. *Nonlinearity*, 11:1209, 1998.
- [9] Predrag Cvitanović. Invariant measurement of strange sets in terms of cycles. *Phys. Rev. Lett.*, 61:2729, 1988.
- [10] P. Dahlqvist. On the effect of pruning on the singularity structure of zeta functions. *J. Math. Phys.*, 38:4273, 1997.
- [11] C. P. Dettmann and P. Cvitanović. Cycle expansions for intermittent diffusion. *Phys. Rev. E*, 56:6687, 1997.
- [12] C. P. Dettmann and T. B. Howard. Asymptotic expansions for the escape rate of stochastically perturbed unimodal maps. *Physica D*, 238:2404, 2009.
- [13] B. Eckhardt and G. Russberg. Resummation of classical and semiclassical periodic-orbit formulas. *Phys. Rev. E*, 47:1578, 1993.
- [14] U. Frisch. *Turbulence*. Cambridge University Press, Cambridge, England, 1996.
- [15] M.C. Gutzwiller. *Chaos in Classical and Quantum Mechanics*. Springer-Verlag, New York, 1990.
- [16] B.-L. Hao. *Chao II*. World Scientific, Singapore, 1990.
- [17] S. Hatjispyros and F. Vivaldi. A family of rational zeta functions for the quadratic map. *Nonlinearity*, 8:321, 1995.
- [18] D. Belkić J. Main, P. A. Dando and H. S. Taylor. Semiclassical quantization by Padé approximant to periodic orbit sums. *Europhys. Lett.*, 48:250, 1999.
- [19] S. F. Nielsen, P. Dahlqvist, and P. Cvitanović. Periodic orbit sum rules for billiards: accelerating cycle expansions. *J. Phys. A: Math. Gen.*, 32:6757, 1999.
- [20] M. L. V. Quyen, J. Martinerie, C. Adam, and F. J. Varela. Unstable periodic orbits in human epileptic activity. *Phys. Rev. E*, 56:3401, 1997.
- [21] H. H. Rugh. The correlation spectrum for hyperbolic analytic maps. *Nonlinearity*, 5:1237, 1992.
- [22] Y. G. Sinai. *Introduction to Ergodic Theory*. Princeton University Press, Princeton, 1976.
- [23] P. So, J. T. Francis, T. I. Netoff, B. J. Gluckman, and S. J. Sciff. Periodic orbits: a new language for neuronal dynamics. *Biophys. J.*, 74:2776, 1998.
- [24] J. Theiler and L. A. Smith. Anomalous convergence of Lyapunov exponent estimates. *Phys. Rev. E*, 51:3738, 1995.